Hindawi
Journal of Chemistry
Volume 2020, Article ID 7512737, 6 pages
https://doi.org/10.1155/2020/7512737

Research Article

Potential Functions and Thermodynamic Properties of UC, UN, and UH

Shuang-Ling Tang,[1] Yu Wang,[1] Qi-Ying Xia ,[2] and Xue-Hai Ju [1]

[1]*School of Environmental and Biochemical Engineering, School of Chemical Engineering, Nanjing University of Science and Technology, 210094 Nanjing, China*
[2]*School of Chemistry and Chemical Engineering, Linyi University, 276005 Linyi, China*

Correspondence should be addressed to Qi-Ying Xia; xiaqiying@163.com and Xue-Hai Ju; xhju@njust.edu.cn

Received 19 October 2019; Accepted 9 January 2020; Published 30 January 2020

Academic Editor: Teik-Cheng Lim

Potential energy surface scanning for UC, UN, and UH was performed by configuration interaction (CI), coupled cluster singles and doubles (CCSD) excitation, quadratic configuration interaction (QCISD (T)), and density functional theory PBE1 (DFT-PBE1) methods in coupling with the ECP80MWB_AVQZ + 2f basis set for uranium and 6 − 311 + G* for carbon, hydrogen, and nitrogen. The dissociation energies of UC, UN, and UH are 5.7960, 4.5077, and 2.6999 eV at the QCISD (T) levels, respectively. The calculated energy was fitted to the potential functions of Morse, Lennard-Jones, and Rydberg by using the least square method. The anharmonicity constant of UC is 0.0047160. The anharmonic frequency of UC is 780.27 cm^{-1} which was obtained based on the PBE1 results. For UN, the anharmonicity constant is 0.0049827. The anharmonic frequency is 812.65 cm^{-1} which was obtained through the PBE1 results. For UH, the anharmonicity constant is 0.017300. The anharmonic frequency obtained via the QCISD (T) results is 1449.8 cm^{-1}. The heat capacity and entropy in different temperatures were calculated using anharmonic frequencies. These properties are in good accordance with the direct DFT-UPBE1 results (for UC and UN) and QCISD (T) results (for UH). The relationship of entropy with temperature was established.

1. Introduction

Among various theoretical simulation methods for molecules and materials, the first principles and molecular dynamic simulation techniques are very powerful for computing the micro and macro properties [1, 2]. The properties and phenomena in materials typically occur at multiple time and length scales. Therefore, to investigate the dynamic behaviors and the time evolution processes, one should resort to the molecular dynamics simulations instead of the first principles [3]. As an alternative solution, molecular dynamics simulation with a molecular force field is a practical method to calculate the dynamic property of the condensed materials [4]. The molecular dynamics uses the Hamilton canonical equation to describe the object system instead of the Schrodinger equation, which requires much smaller computational resources. Furthermore, the kinetic degrees of freedom are easily traversed to obtain the normal frequencies and thus obtain the thermodynamic properties [5]. The computational scale of molecular dynamics methods are on the nanometer and nanosecond scales [6–8]. Consequently, the development of the simulation techniques that couple together with physics on multiple levels is of very importance. In order to realize this goal, one should develop an atom-atom pair potential and obtain the parameters of the force field. The characteristics of the potential energy between diatomic molecules can be described by the corresponding analytical potential energy functions [9]. In particular, the potential function is necessary for establishing and optimizing the force field parameters, which in turn plays an important role for investigating static and dynamic properties of molecules as well as of solid states [10, 11].

The molecular dynamics deals with the atom-to-atom forces and the individual atomic movement. It is equally applicable for both crystalline and noncrystalline materials. Furthermore, molecular dynamics could obtain the total energy composed of all interatomic potential energies and kinetic energies of all degrees of freedom at any loading and temperature conditions. The initial important step in molecular dynamics simulations is the selection of interatomic potentials. For metals, the Morse potential is the most popular one [9, 12]. However, the interatomic potentials or the force field parameters are not available in the commonly used COMPASS force field for the uranium atom except for its oxides. In this paper, we scanned the potential energy surface of UC, UN, and UH with *ab initio* configuration interaction (CI), coupled cluster singles and doubles (CCSD) excitation, quadratic configuration interaction (QCISD (T)), and density functional theory PBE1 methods [13]. Then, the Morse potential functions were established. We also fit the energy curves into the Lennard-Jones (L-J) and Rydberg potentials. The thermodynamic properties were calculated by using the Morse potential parameters in a temperature of 298.2 K to 1500 K. For comparison, the heat capacity and entropy were also obtained with the usage of the DFT-PBE1 or QCISD (T) methods.

2. Computational Methods

Computational methods usually produce more accurate results when the higher level method is used. However, it is computationally too expensive or impractical to use methods such as CASSCF to establish the potential energy surface of UC, UN, and UH. Then, we selected the less expensive *ab initio* CI, CCSD, QCISD (T), and DFT-PBE1 methods to determine the potential energy surface. The calculations described in this paper were performed with the Gaussian 09 package [14]. The DFT method is at the PBE1 level. The basis sets for uranium is ECP80MWB_AVQZ + 2f and $6-311+G^*$ for carbon, nitrogen, and hydrogen [15]. The basis set of ECP80MWB_AVQZ + 2f includes a quasirelativistic effective core potential, which represents the relativistic effects largely confined to the core, and an augmented correlation consistent valence quadruple aug-cc-pVQZ (AVQZ level) basis set [16] for the valence, together with 2f in the valence. As a whole, the results from the f-in-core and f-in-valence pseudopotentials are in good agreement [17], and the quality of AVQZ is so good that it is comparable to the complete basis set (CBS) in most cases. This basis set guarantees its well behavior for U. The CI, CCSD, QCISD (T), and DFT methods are reliable for the investigation of transition metal compounds [18, 19]. After the potential energies being obtained, a Morse function was fit as follows:

$$U(r) = D_e\left(e^{-2\beta(r-r_0)} - 2e^{-\beta(r-r_0)}\right). \quad (1)$$

The eigenvalue of the Morse potential is

$$U(n) = hc\left[(n+0.5)\omega_e - (n+0.5)^2\chi_e\omega_e\right], \quad (2)$$

and

$$\omega_e = \beta\left(\frac{2D_e}{\mu}\right)^{0.5}(2\pi c)^{-1}, \quad (3)$$

$$\chi_e = \frac{\omega_e}{4D_e}, \quad (4)$$

where ω_e is the harmonic vibrational frequency, D_e is the minimum point in the Morse curve that equals to the dissociation energy in a diatomic system, β is a parameter that is related to the width of the Morse potential curve, μ the reduced mass, and χ_e the anharmonic constant. For comparison, we also fit the Lennard-Jones and the Rydberg interatomic potential functions, respectively, as follows:

$$U(r) = \frac{A}{r^{12}} - \frac{B}{r^6},$$
$$U(r) = -D_e(1+\beta r)\cdot\exp(-\beta r). \quad (5)$$

By neglecting the contribution of the electronic energy of the excitation states to its thermodynamic properties, the heat capacity and the entropy were calculated. The heat capacity and entropy were obtained on the basis of the vibrational frequencies from DFT-PBE1 or QCISD (T) calculations and the fitted Morse parameters.

3. Results and Discussion

3.1. Potential Energy. The potential energy surfaces of UC, UN, and UH were obtained by the CCSD, CI, QCISD (T), and DFT-PBE1 methods. It is worth noting that the lowest lying states were selected in the potential energy scanning. The triplet was adopted for UC, and the doublet was adopted for UN and UH after comparing the energies of different multiplicities. For instances, the total energies of UC are −75.22439079 a.u. ($r_0 = 2.25$ Å) and −75.28543016 a.u. ($r_0 = 2.00$ Å) for the heplet and triplet, respectively, at the PBE1 level by using the ECP80MWB_AVQZ + 2f basis set for U and $6-311+G^*$ basis set for carbon. The triplet UC is more stable than its heplet state. The dissociation energies of UC, UN, and UH are 5.7960, 4.5077, and 2.6999 eV at the QCISD (T) levels, respectively.

Table 1 lists the parameters of potential functions of UC, UN, and UH. As can be seen from Table 1, the data from PBE1 were well fitted to the Morse function for UC and UN, in view of larger values of R-square and smaller values of RMSE. However, the best results for UH are from the QCISD (T), which could be well fitted to the Morse or Rydberg functions. Figures 1–3 show the calculated results from PBE1 or QCISD (T) and the fitted Morse curves. As can be seen from these figures, the fitted Morse functions behave almost exactly as the potential energies of PBE1 or QCISD (T). Similarly, the fitted Rydberg functions behave almost as Morse functions. For UC and UN, the Morse functions are slightly better than the Rydberg functions, but the latter is slightly better for UH judged by the values of *R*-square and RMSE. However, the correlation coefficients for the fitted Lennard-Jones functions are in the range of 0.6199 to 0.9253, and root mean square errors are in range of 1.326 to 3.608 eV, indicating the L-J is not a good model for UC, UN,

Table 1: Parameters of potential functions of UC, UN, and UH[a].

Compound	Function	Methods	Parameters		R-square	RMSE
UC	Morse	CI	$D_e = 5.153$	$\beta = 1.47$	0.9913	0.6759
		PBE1	$D_e = 5.152$	$\beta = 1.583$	0.9988	0.2734
		CCSD	$D_e = 6.269$	$\beta = 1.508$	0.9911	0.8428
		QCISD (T)	$D_e = 6.387$	$\beta = 1.501$	0.9916	0.8534
	L-J	CI	$A = 97.4$	$B = -32.43$	0.8713	2.6000
		PBE1	$A = 88.4$	$B = -40.76$	0.8832	2.6440
		CCSD	$A = 100.5$	$B = -34.77$	0.8489	3.4820
		QCISD (T)	$A = 101$	$B = -34.45$	0.8505	3.6080
	Rydberg	CI	$D_e = 5.368$	$\beta = 2.135$	0.9901	0.7198
		PBE1	$D_e = 5.333$	$\beta = 2.305$	0.9974	0.3938
		CCSD	$D_e = 6.424$	$\beta = 2.197$	0.9881	0.9788
		QCISD (T)	$D_e = 6.551$	$\beta = 2.186$	0.9889	0.9840
UN	Morse	CI	$D_e = 3.161$	$\beta = 2.535$	0.9736	1.2290
		PBE1	$D_e = 5.08$	$\beta = 1.79$	0.9972	0.3866
		CCSD	$D_e = 4.197$	$\beta = 2.06$	0.9585	1.5640
		QCISD (T)	$D_e = 4.186$	$\beta = 2.031$	0.9887	0.8275
	L-J	CI	$A = 111.1$	$B = -32.01$	0.9253	2.0670
		PBE1	$A = 130.7$	$B = -18.98$	0.8864	2.4540
		CCSD	$A = 114.2$	$B = -30.18$	0.9201	2.1710
		QCISD (T)	$A = 115.4$	$B = -29.58$	0.9159	2.2540
	Rydberg	CI	$D_e = 3.951$	$\beta = 3.94$	0.9591	1.5300
		PBE1	$D_e = 5.289$	$\beta = 2.603$	0.9968	0.4096
		CCSD	$D_e = 4.271$	$\beta = 2.977$	0.9584	1.5650
		QCISD (T)	$D_e = 4.422$	$\beta = 2.951$	0.9573	1.6060
UH	Morse	PBE1	$D_e = 2.535$	$\beta = 1.326$	0.9874	0.2750
		CCSD	$D_e = 2.265$	$\beta = 1.29$	0.9859	0.2769
		QCISD (T)	$D_e = 2.643$	$\beta = 1.235$	0.9940	0.1925
	L-J	PBE1	$A = 40.08$	$B = -0.0883$	0.6342	1.4820
		CCSD	$A = 35.27$	$B = -2.884$	0.6777	1.3260
		QCISD (T)	$A = 39.82$	$B = -0.08717$	0.6199	1.5330
	Rydberg	PBE1	$D_e = 2.612$	$\beta = 1.921$	0.9906	0.2371
		CCSD	$D_e = 2.339$	$\beta = 1.87$	0.9885	0.2505
		QCISD (T)	$D_e = 2.707$	$\beta = 1.79$	0.9950	0.1751

[a]Unit of D_e and RMSE is eV, the unit of β is $Å^{-1}$, and the units of A and B are eV•$Å^{12}$ and eV•$Å^6$.

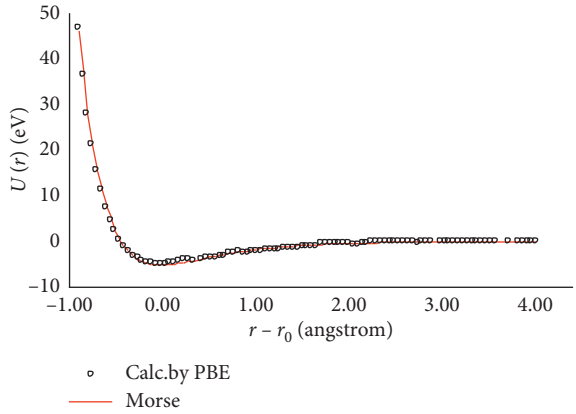

Figure 1: Potential energy vs. diatomic distance for UC.

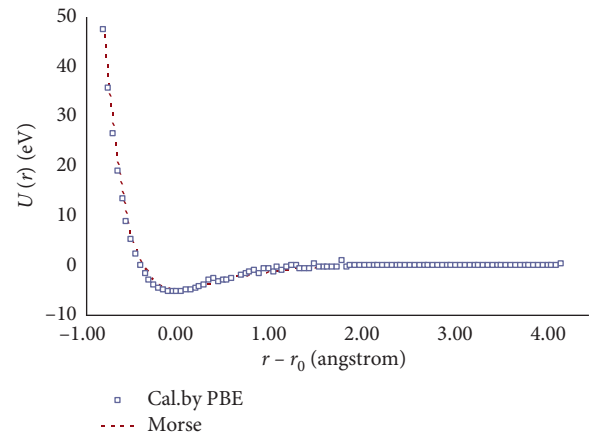

Figure 2: Potential energy vs. diatomic distance for UN.

and UH potentials. The L-J potential is generally good approximation to describe the dispersion and overlap interactions in molecules. However, it is not good to a strong U-X bond, since the twelfth-power repulsive term appearing in the Lennard-Jones potential is chosen for its ease of calculation for simulations (by squaring the sixth-power term) and is not physically based. For brevity, only the drawings from the Morse functions are shown in Figures 1–3. In addition, the potential curve from the CI method is not continuous for UH. Its potential drops all of a sudden at $r = 6.3$ Å, indicating that the CI method is not applicable for UH. Therefore, we did not apply this method to establish a potential function for the UH system.

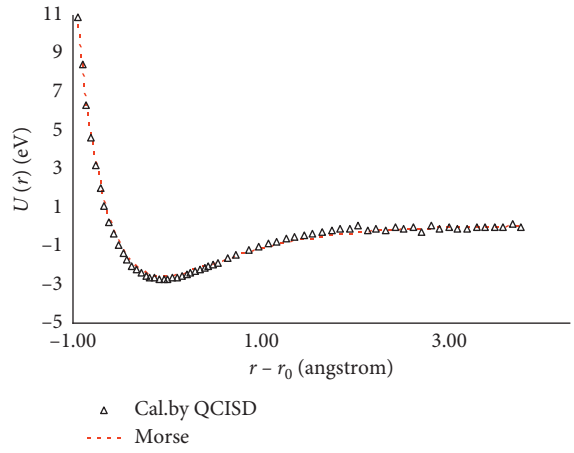

Figure 3: Potential energy vs. diatomic distance for UH.

For UC, the values of D_e and β of the Morse function fitted from DFT-PBE1 results are 5.152 eV and 1.583 Å^{-1}, respectively. Thus, $\omega_e = 783.97\ \text{cm}^{-1}$ after substituting the β and D_e values into equation (3). By substituting these values into equation (4), the anharmonicity constant $\chi_e = 0.004716$ and $\chi_e\omega_e = 3.70\ \text{cm}^{-1}$. The anharmonic frequency is $780.27\ \text{cm}^{-1}$, which is slightly smaller than the scaled frequency ($831.58\ \text{cm}^{-1}$) obtained from DFT-PBE1 when it is scaled by a factor of 0.96.

For UN, the values of D_e and β of the Morse function fitted from DFT-PBE1 results are 5.08 eV and 1.79 Å^{-1}, respectively. Thus, $\omega_e = 816.72\ \text{cm}^{-1}$ after substituting the β and D_e values into equation (3). Then, the anharmonicity constant $\chi_e = 0.004983$ from equation (4), and $\chi_e\omega_e = 4.07\ \text{cm}^{-1}$. The anharmonic frequency is $812.65\ \text{cm}^{-1}$, which is also slightly smaller than the scaled frequency ($887.18\ \text{cm}^{-1}$) obtained from DFT-PBE1 when it is scaled by a factor of 0.96.

For UH, the values of D_e and β of the Morse function fitted from QCISD (T) results are 2.643 eV and 1.235 Å^{-1}, respectively. Thus, $\omega_e = 1475.3\ \text{cm}^{-1}$ after substituting the β and D_e values into equation (3). Consequently, the anharmonicity constant $\chi_e = 0.01730$ from equation (4) and $\chi_e\omega_e = 25.5\ \text{cm}^{-1}$. The $\chi_e\omega_e$ value of UH is much larger than that of UC or UN. The anharmonic frequency of UH is $1449.8\ \text{cm}^{-1}$, which is slightly smaller than the scaled frequency ($1468.46\ \text{cm}^{-1}$) obtained from QCISD (T) after being scaled by a factor of 0.96. Luo et al. [20] used the B3LYP/SDD method to derive $D_e = 2.886$ eV and $\omega_e = 1540.403\ \text{cm}^{-1}$, which are close to our results. Since the SDD basis set is small and the RMSE from the DFT method is larger than that from QCISD (T) (Table 1), our results are expected to be more reliable.

3.2. Thermodynamic Properties. Tables 2–4 list the entropy and heat capacity of UC, UN, and UH, respectively, in a temperature of 298.2 K to 1500 K. The results from the Morse potentials for UC and UN are almost identical to those of DFT-PBE1 calculations. The results from Morse and QCISD are similar for UH. The C_P values increase very slightly with increasing temperature. The entropies also increase as temperature rises. The relationship between entropy and temperature can be fitted as a linear equation

Table 2: Entropy and heat capacity of UC.

Temp. (K)	DFT-PBE1		Morse	
	C_P (J/mol/K)	S (J/mol/K)	C_P (J/mol/K)	S (J/mol/K)
298.2	31.60	239.09	31.96	239.26
400.0	33.24	248.61	33.58	248.89
500.0	34.36	256.16	34.65	256.51
600.0	35.13	262.49	35.36	262.89
700.0	35.65	267.95	35.84	268.38
800.0	36.02	272.73	36.18	273.19
900.0	36.29	276.99	36.42	277.46
1000.0	36.49	280.82	36.60	281.31
1100.0	36.64	284.31	36.73	284.80
1200.0	36.76	287.50	36.84	288.00
1300.0	36.85	290.44	36.92	290.95
1400.0	36.93	293.18	36.98	293.69
1500.0	36.99	295.73	37.04	296.24

Table 3: Entropy and heat capacity of UN.

Temp. (K)	DFT-PBE1		Morse	
	C_P (J/mol/K)	S (J/mol/K)	C_P (J/mol/K)	S (J/mol/K)
298.2	31.26	239.34	31.74	239.55
400.0	32.88	248.76	33.37	249.12
500.0	34.06	256.23	34.48	256.69
600.0	34.87	262.51	35.22	263.04
700.0	35.45	267.93	35.73	268.51
800.0	35.85	272.69	36.08	273.30
900.0	36.15	276.93	36.34	277.57
1000.0	36.37	280.75	36.53	281.41
1100.0	36.54	284.22	36.68	284.89
1200.0	36.67	287.41	36.79	288.09
1300.0	36.78	290.35	36.88	291.04
1400.0	36.86	293.08	36.95	293.77
1500.0	36.93	295.62	37.01	296.32

Table 4: Entropy and heat capacity of UH.

Temp. (K)	QCISD*		Morse	
	C_P (J/mol/K)	S (J/mol/K)	C_P (J/mol/K)	S (J/mol/K)
298.2	29.46	217.97	29.46	217.97
400.0	30.32	226.74	30.31	226.74
500.0	31.37	233.61	31.36	233.61
600.0	32.37	239.42	32.36	239.41
700.0	33.23	244.48	33.22	244.47
800.0	33.93	248.96	33.92	248.95
900.0	34.49	252.99	34.48	252.98
1000.0	34.93	256.65	34.93	256.63
1100.0	35.29	259.99	35.29	259.98
1200.0	35.59	263.07	35.58	263.06
1300.0	35.82	265.93	35.82	265.92
1400.0	36.02	268.59	36.01	268.58
1500.0	36.18	271.08	36.18	271.07

*As the frequency computation was not executed in G09 software for the QCISD (T) method, we instead used the frequencies from QCISD.

with large correlation coefficient. From the Morse results and DFT-PBE1 results of UC, the established equations are $S = 264.6 + 0.0262\,T - 10150.0\,T^{-1}$ and $S = 263.9 + 0.02624\,T - 10010.0T^{-1}$, respectively. The correlation coefficient R^2 is 0.999 for both, with a root mean square error of 0.694 J mol^{-1} K^{-1} for both Morse and DFT-PBE1 results. From the Morse results and DFT-PBE1 results of UN, the established equations are $S = 264.6 + 0.02623\,T - 10060\,T^{-1}$ and $S = 263.7 + 0.02626\,T - 9859\,T^{-1}$, respectively. The correlation coefficient R^2 is 0.999 for both, with a root mean square error of 0.692 J mol^{-1} K^{-1} for Morse results and 0.687 J mol^{-1} K^{-1} for DFT-PBE1 results. From the Morse results and QCISD results of UH, the established equations are $S = 239.1 + 0.02575\,T - 8818\,T^{-1}$ and $S = 263.7 + 0.02626\,T - 9859\,T^{-1}$, respectively. The correlation coefficient R^2 is 0.999 for both, with a root mean square error of 0.596 J mol^{-1} K^{-1} for Morse results and 0.598 J mol^{-1} K^{-1} for QCISD results.

4. Conclusions

Many conventional and standard basis sets fail to converge and/or produce irrational results for the U-containing system. The basis set of ECP80MWB_AVQZ + 2f is a well behaved basis set for U. The anharmonicity constant of UC and UN is small, but that of UH is large. The Morse function is suitable for the UC, UN, and UH potentials, so is the Rydberg function. The entropy and heat capacity of UC and UN in a temperature of 298.2 K to 1500 K from the Morse potential are close to those from the DFT-PBE1 results. The entropy and heat capacity of UH from the Morse potential are comparable to those from QCISD (T). The C_P values increase slightly, but the entropies increase greatly with increasing temperature for UC, UN, and UH. The predicted functions provided useful parameters for establishing the force field of the U-containing system.

Data Availability

The data used to support the findings of this study are available from the corresponding author upon request.

Conflicts of Interest

The authors declare no conflicts of interest.

Authors' Contributions

Xue-Hai Ju conceptualized the study; Shuang-Ling Tang and Yu Wang were involved in data curation; Xue-Hai Ju was responsible for project administration; Qi-Ying Xia was involved resource management; Shuang-Ling Tang wrote the original draft; and Xue-Hai Ju and Qi-Ying Xia wrote, reviewed, and edited the manuscript.

Acknowledgments

This work was financially supported by the National Science Foundation of China (Grant no. 21101070).

References

[1] X. W. Wu and B. R. Brooks, "A double exponential potential for van der Waals interaction," *AIP Advances*, vol. 9, no. 6, Article ID 065304, 2019.

[2] C.-F. Li, Z. Mei, F.-Q. Zhao, S.-Y. Xu, and X.-H. Ju, "Molecular dynamic simulation for thermal decomposition of RDX with nano-AlH_3 particles," *Physical Chemistry Chemical Physics*, vol. 20, no. 20, pp. 14192–14199, 2018.

[3] S. Mukherjee, S. Mondal, and B. Bagchi, "Mechanism of solvent control of protein dynamics," *Physical Review Letters*, vol. 122, no. 5, Article ID 058101, 2019.

[4] E. Martínez, R. Perriot, E. M. Kober et al., "Parallel replica dynamics simulations of reactions in shock compressed liquid benzene," *The Journal of Chemical Physics*, vol. 150, no. 24, Article ID 244108, 2019.

[5] J. Yuan, L. Zhong, M. Vakili, and G. A. Segun, "New modeling method to simulate asphaltenes at oil sands process in water management," *Journal of Molecular Graphics and Modelling*, vol. 91, pp. 1–9, 2019.

[6] D. Wang and P. E. Marszalek, "All-atom steered molecular dynamics simulations of large proteins in a small water box," *Biophysical Journal*, vol. 116, no. 3, p. 326a, 2019.

[7] C. Scherer, F. Schmid, M. Letz, and J. Horbach, "Structure and dynamics of B_2O_3 melts and glasses: from ab initio to classical molecular dynamics simulations," *Computational Materials Science*, vol. 159, pp. 73–85, 2019.

[8] A. Gijón, A. Lasanta, and E. R. Hernández, "Paths towards equilibrium in molecular systems: the case of water," *Physical Review E*, vol. 100, no. 3, Article ID 032103, 2019.

[9] H. Y. Abdullah, "A comparative study of potential energy curves with RKRV curves for the ground states of I_2, F_2 and CO molecules," *Bulletin of Materials Science*, vol. 42, no. 4, p. 142, 2019.

[10] K. R. Sun, K. Y. Zhao, L. Li, Y. F. Guo, and T. L. Deng, "Heat capacity and thermodynamic property of cesium tetraborate pentahydrate," *Journal of Chemistry*, vol. 2019, Article ID 71328, 5 pages, 2019.

[11] J. A. Harrison, J. D. Schall, S. Maskey, P. T. Mikulski, M. T. Knippenberg, and B. H. Morrow, "Review of force fields and intermolecular potentials used in atomistic computational materials research," *Applied Physics Reviews*, vol. 5, no. 3, Article ID 031104, 2018.

[12] A. A. Medvedev, V. V. Meshkov, A. V. Stolyarov, and M. C. Heaven, "Ab initio interatomic potentials and transport properties of alkali metal (M = Rb and Cs)-rare gas (Rg = He, Ne, Ar, Kr, and Xe) media," *Physical Chemistry Chemical Physics*, vol. 20, no. 40, pp. 25974–25982, 2018.

[13] J. B. Foresman and A. E. Frisch, *Exploring Chemistry with Electroinc Structure Methods*, Gaussian Inc., Pittsburgh, PA, USA, 1996.

[14] M. J. Frisch, G. W. Trucks, H. B. Schlegel et al., *Gaussian 09, Revision A.02*, Gaussian Inc., Pittsburgh, PA, USA, 2009.

[15] A. Moritz, X. Cao, and M. Dolg, "Quasirelativistic energy-consistent 5f-in-core pseudopotentials for divalent and tetravalent actinide elements," *Theoretical Chemistry Accounts*, vol. 118, no. 5-6, pp. 845–854, 2007.

[16] D. E. Woon and T. H. Dunning, "Gaussian basis sets for use in correlated molecular calculations. III. The atoms aluminum through argon," *The Journal of Chemical Physics*, vol. 98, no. 2, pp. 1358–1371, 1993.

[17] A. Weigand, X. Cao, J. Yang, and M. Dolg, "Quasirelativistic f-in-core pseudopotentials and core-polarization potentials for trivalent actinides and lanthanides: molecular test for

trifluorides," *Theoretical Chemistry Accounts*, vol. 126, no. 3-4, pp. 117–127, 2010.

[18] T. V. Harris and R. K. Szilagyi, "Iron-sulfur bond covalency from electronic structure calculations for classical iron-sulfur clusters," *Journal of Computational Chemistry*, vol. 35, no. 7, pp. 540–552, 2014.

[19] S. T. Disale, C. V. S. Brahmmananda Rao, G. Gopakumar, and R. V. Jayaram, "Experimental and theoretical studies on actinide extraction: dibutyl phenyl phosphonate versus tri-n-butyl phosphate," *Journal of Coordination Chemistry*, vol. 72, no. 9, pp. 1480–1496, 2019.

[20] D. L. Luo, Y. Sun, X. Y. Liu, G. Jiang, D. Q. Meng, and Z. H. Zhu, "Structure and potential energy function investigation on UH and UH_2 molecules," *Acta Physica Sinica*, vol. 50, pp. 1896–1901, 2001.